

## Article

# Lung Nodules Missed in Initial Staging of Breast Cancer Patients in PET/MRI—Clinically Relevant?

Kai Jannusch <sup>1</sup>, Nils Martin Bruckmann <sup>1</sup>, Charlotte Johanna Geuting <sup>1</sup>, Janna Morawitz <sup>1</sup>, Frederic Dietzel <sup>1</sup>, Christoph Rischpler <sup>2</sup>, Ken Herrmann <sup>2</sup>, Ann-Kathrin Bittner <sup>3</sup>, Oliver Hoffmann <sup>3</sup>, Svetlana Mohrmann <sup>4</sup>, Harald H. Quick <sup>5,6</sup>, Lale Umutlu <sup>7</sup>, Gerald Antoch <sup>1</sup> and Julian Kirchner <sup>1,\*</sup>

<sup>1</sup> Department of Diagnostic and Interventional Radiology, Medical Faculty, University Dusseldorf, 40225 Dusseldorf, Germany; kai.jannusch@med.uni-duesseldorf.de (K.J.); nils-martin.bruckmann@med.uni-duesseldorf.de (N.M.B.); charlotte.geuting@gmx.de (C.J.G.); janna.morawitz@med.uni-duesseldorf.de (J.M.); frederic.dietzel@med.uni-duesseldorf.de (F.D.); antoch@med.uni-duesseldorf.de (G.A.)

<sup>2</sup> Department of Nuclear Medicine, University Hospital Essen, University of Duisburg-Essen, 45147 Essen, Germany; christoph.rischpler@uk-essen.de (C.R.); ken.herrmann@uk-essen.de (K.H.)

<sup>3</sup> Department Gynecology and Obstetrics, University Hospital Essen, University of Duisburg-Essen, 45147 Essen, Germany; ann-kathrin.bittner@uk-essen.de (A.-K.B.); oliver.hoffmann@uk-essen.de (O.H.)

<sup>4</sup> Department of Gynecology, Medical Faculty, University Dusseldorf, 40225 Dusseldorf, Germany; mohrmann@med.uni-duesseldorf.de

<sup>5</sup> High-Field and Hybrid MR Imaging, University Hospital Essen, University Duisburg-Essen, 45147 Essen, Germany; harald.quick@uk-essen.de

<sup>6</sup> Erwin L. Hahn Institute for Magnetic Resonance Imaging, University Duisburg-Essen, 45141 Essen, Germany

<sup>7</sup> Department of Diagnostic and Interventional Radiology and Neuroradiology, University Hospital Essen, University of Duisburg-Essen, 45147 Essen, Germany; lale.umutlu@uk-essen.de

\* Correspondence: julian.kirchner@med.uni-duesseldorf.de; Tel.: +49-211-8-11-77-54



**Citation:** Jannusch, K.; Bruckmann, N.M.; Geuting, C.J.; Morawitz, J.; Dietzel, F.; Rischpler, C.; Herrmann, K.; Bittner, A.-K.; Hoffmann, O.; Mohrmann, S.; et al. Lung Nodules Missed in Initial Staging of Breast Cancer Patients in PET/MRI—Clinically Relevant?. *Cancers* **2022**, *14*, 3454. <https://doi.org/10.3390/cancers14143454>

Academic Editor: Angela Spanu

Received: 8 June 2022

Accepted: 14 July 2022

Published: 15 July 2022

**Publisher's Note:** MDPI stays neutral with regard to jurisdictional claims in published maps and institutional affiliations.



**Copyright:** © 2022 by the authors. Licensee MDPI, Basel, Switzerland. This article is an open access article distributed under the terms and conditions of the Creative Commons Attribution (CC BY) license (<https://creativecommons.org/licenses/by/4.0/>).

**Simple Summary:** Image-based primary staging in women with newly-diagnosed breast cancer is important to exclude distant metastases, which affect up to 10% of women. The increasing implementation of [<sup>18</sup>F]FDG-PET/MRI as a radiation-saving primary staging tool bears the risk of missing lung nodules. Thus, chest CT serves as the diagnostic of choice for the detection and classification of pulmonary nodules. The aim of this study was the evaluation of the clinical relevance of missed lung nodules at initial staging of breast cancer patients in [<sup>18</sup>F]FDG-PET/MRI compared with CT. We demonstrated in an homogeneous population of 152 patients that all patients with newly-diagnosed breast cancer and clinically-relevant lung nodules were detected at initial [<sup>18</sup>F]FDG-PET/MRI staging. However, due to the lower sensitivity of MRI in detecting lung nodules, a small proportion of clinically-relevant lung nodules were missed. Thus, a supplemental low-dose chest CT after neoadjuvant therapy should be considered for backup.

**Abstract:** Purpose: The evaluation of the clinical relevance of missed lung nodules at initial staging of breast cancer patients in [<sup>18</sup>F]FDG-PET/MRI compared with CT. Methods: A total of 152 patients underwent an initial whole-body [<sup>18</sup>F]FDG-PET/MRI and a thoracoabdominal CT for staging. Presence, size, shape and location for each lung nodule in [<sup>18</sup>F]FDG-PET/MRI was noted. The reference standard was established by taking initial CT and follow-up imaging into account (a two-step approach) to identify clinically-relevant lung nodules. Patient-based and lesion-based data analysis was performed. Results: No patient with clinically-relevant lung nodules was missed on a patient-based analysis with MRI VIBE, while 1/84 females was missed with MRI HASTE (1%). Lesion-based analysis revealed 4/96 (4%, VIBE) and 8/138 (6%, HASTE) missed clinically-relevant lung nodules. The average size of missed lung nodules was 3.2 mm ± 1.2 mm (VIBE) and 3.6 mm ± 1.4 mm (HASTE) and the predominant location was in the left lower quadrant and close to the hilum. Conclusion: All patients with newly-diagnosed breast cancer and clinically-relevant lung nodules were detected at initial [<sup>18</sup>F]FDG-PET/MRI staging. However, due to the lower sensitivity in detecting lung nodules, a small proportion of clinically-relevant lung nodules were missed. Thus, supplemental low-dose chest CT after neoadjuvant therapy should be considered for backup.

**Keywords:** PET/MRI; breast cancer; lung nodules; staging

## 1. Introduction

Breast cancer is the most common solid tumor in women worldwide, accounting for 11.7% of all cancers diagnoses and approximately 2.3 million new cases every year [1]. In addition to knowledge of tumor biology, accurate knowledge of the TNM stage is essential for therapy planning [2,3]. Therefore, imaging plays a key role in the diagnostic workup of breast cancer patients. Current guidelines recommend chest/abdomen computed tomography (CT) and bone scintigraphy for staging. Especially in unequivocal cases, <sup>18</sup>F-fluorodeoxyglucose (<sup>18</sup>F]FDG) Positron emission tomography (PET)/CT can be used as a supporting diagnostic tool [4,5]. Furthermore, some studies suggest performing initial staging with PET/CT in predefined patient groups [5–7]. As an alternative to PET/CT, PET/magnet resonance imaging (MRI) is gaining visibility as a staging method for breast cancer patients by combining high-quality whole-body staging and multiparametric breast MRI, and has shown its superiority over PET/CT, MRI and CT [8–11]. However, detecting small lung nodules remains a major problem in MRI, and CT is still the golden standard for lung evaluation. One reason for this is the susceptibility of MRI to respiratory and cardiac motion resulting in a markedly reduced accessibility of the lung parenchyma and limited detectability of potentially metastatic lung nodules [12]. Despite technical advances in MR imaging over the years, several studies showed that lung nodules, especially small ones, continue to be missed [12–14]. In general, interpreting small lung nodules represents a problem in radiological diagnostics. Even though the majority of these lung nodules are benign (i.e., post-infectious or indurative genesis), it is important to ensure that no malignant lung nodules are missed [15,16]. Thus, a clinically-balanced staging is necessary which, on the one hand, does not negate any relevant findings; but, on the other hand, does not lead to an unjustified upstaging or follow-up imaging. For this purpose, the current Fleischner Society recommendations provide clinically-accepted guidelines on how to deal with small pulmonary nodules by recommending follow-up examination for nodules > 6 mm at different time intervals, depending on size, morphology, and patients history [17].

The aim of this study was to evaluate the clinical relevance of missed lung nodules at initial staging of breast cancer patients in [<sup>18</sup>F]FDG-PET/MRI compared with CT.

## 2. Materials and Methods

### 2.1. Patients

The institutional review boards of the University Duisburg-Essen, Germany (study number 17-7396-BO) and Düsseldorf, Germany (study number 6040 R) approved this study, and it was performed in conformance with the Declaration of Helsinki [18]. Written informed consent form was obtained from all patients. Inclusion criteria were defined as follows: (1) newly diagnosed, treatment-naive T2 tumor or higher T-stage; or (2) newly diagnosed, treatment-naive triple-negative tumor of every size; or (3) newly diagnosed, treatment-naive tumor with molecular high risk (T1 c, Ki67 > 14%, HER2-new over-expression, G3). Exclusion criteria were contraindications to MRI or MRI contrast agents, missing imaging of a modality, pregnancy or breast-feeding and former malignancies in the last 5 years. Inclusion criteria were chosen according to clinical ESMO guidelines to set elevated pre-test probability for distant metastases [19,20]. Data acquisition was performed between March 2018 and December 2021.

A total of 152 women with newly-diagnosed breast cancer (mean age: 53 years ± 12 years; range 30–81 years) were included in this study. As part of this study all women underwent a whole-body [<sup>18</sup>F]FDG-PET/MRI examination for staging purposes in addition to a thoraco-abdominal CT with a maximum of 30 days apart (mean:

5.2 days  $\pm$  5.4 days). Due to cohort size, no further subgroup analyses was performed regarding different cancer subtypes.

## 2.2. PET/MRI

All [ $^{18}\text{F}$ ]FDG-PET/MRI examinations were performed on an integrated 3-Tesla PET/MRI system (Biograph mMR, Siemens Healthcare GmbH, Erlangen, Germany). Examinations were performed one hour after injection of bodyweight-adapted dosage of [ $^{18}\text{F}$ ]FDG (4 MBq/kg bodyweight). The imaging protocol included a dedicated breast [ $^{18}\text{F}$ ]FDG-PET/MRI and a whole-body imaging scan [21]. Only the whole-body PET/MR examinations were considered for this study. [ $^{18}\text{F}$ ]FDG-PET images were reconstructed after a standard protocol [22]. MRI data were acquired simultaneously using a 16-channel head-and-neck radiofrequency (RF) coil, a 24-channel spine array RF coil and 5 or 6-channel flex body coils, depending on patients' height. The WB-MRI protocol comprised the following sequences:

- i. A transverse T2-w half Fourier acquisition single shot turbo spin echo (HASTE) sequence in breath-hold technique with a slice thickness of 7 mm (TE 97 ms; TR 1500 ms; turbo factor (TF) 194; FOV 400 mm; phase FOV 75%; acquisition matrix 320  $\times$  240 mm; in plane resolution 1.3  $\times$  1.3 mm; TA 0:47 min/bed position)
- ii. A fat-saturated post-contrast transverse 3-dimensional volumetric interpolated breath-hold examination (VIBE) sequence with a slice thickness of 3 mm (TE, 1.53 ms; TR, 3.64 ms; flip angle 9°; FOV 400  $\times$  280 mm; phase FOV 75%; acquisition matrix 512  $\times$  384, in-plane resolution 0.7  $\times$  0.7 mm; TA 0:19 min/bed position)
- iii. A transversal diffusion-weighted (DW) echo-planar imaging (EPI) sequence in free breathing with a slice thickness of 5.0 mm (TR 7400 ms; TE 72 ms; b-values: 0, 500, and 1000 s/mm<sup>2</sup>, matrix size 160  $\times$  90; FOV 400 mm  $\times$  315 mm, phase FOV, 75%; GRAPPA, acceleration factor 2; in-plane resolution 2.6  $\times$  2.6 mm; TA 2:06 min/bed position).

## 2.3. Computed Tomography

CT examinations were performed on a dedicated CT system (Siemens Flash or Siemens Somatom AS, Siemens Healthcare GmbH, Erlangen, Germany) using automated tube current modulation and automated tube voltage selection (CareDose 4 D and CareKV, Siemens Healthcare GmbH). A bodyweight-adapted dosage of iodinated contrast medium was administered intravenously 70 s before the scan. Thoracic images were reconstructed in the lung window setting, using a sharp kernel (B70 s) and a slice thickness of 2 mm.

## 2.4. Image Analysis

The chest imaging datasets of the [ $^{18}\text{F}$ ]FDG-PET/MRI examination and CT were analysed on a dedicated OsiriX workstation (Pixmeo, SARL, Bernex, Switzerland) by two experienced radiologists in a random order and in separate sessions, with at least two weeks apart to avoid recognition bias. Any discrepancies between the two readers were resolved in a subsequent consensus reading. In PET/MRI, the VIBE and HASTE sequence were evaluated both independently of one another and considered together. None of the missed lung nodules showed a FDG uptake in the [ $^{18}\text{F}$ ]FDG-PET component.

Both readers were informed regarding the primary diagnosis of the patients but remained blind to the results of prior and follow-up imaging and to the patients' histories.

The quality of all thoracic imaging datasets was evaluated on a four-point Likert scale to differentiate between (1) very poor image quality with major artifacts, (2) poor image quality with moderate artifacts, (3) good image quality with minor artifacts and (4) excellent image quality without any artifacts. The presence and type of artifacts was documented. Lungs were systematically assessed in the same order, dividing the lungs into a (1) right upper, (2) left upper, (3) right lower and (4) left lower quadrant. The amount of lung nodules and the location was noted. Further lung sections were subdivided into a pleural, a subpleural (max. of 1 cm distance to pleura), a central and a hilus region. Nodule size was measured at long axis in mm. Furthermore, nodule contrast was categorized

by (1) very low contrast, (2) low contrast, (3) moderate contrast and (4) high contrast. Nodule density was divided into (1) solid, (2) part-solid and (3) pure ground glass (see Figure 1). The nodule shape was classified into (1) round, (2) oval, (3) ellipsoid, (4) lobular, (5) notched and (6) irregular. Initially, a maximum of 10 lung nodules was identified for each patient on baseline imaging. Subsequently, every lung nodule was classified as (1) benign, (2) follow-up needed or (3) malign according, to the actual Fleischner guidelines.

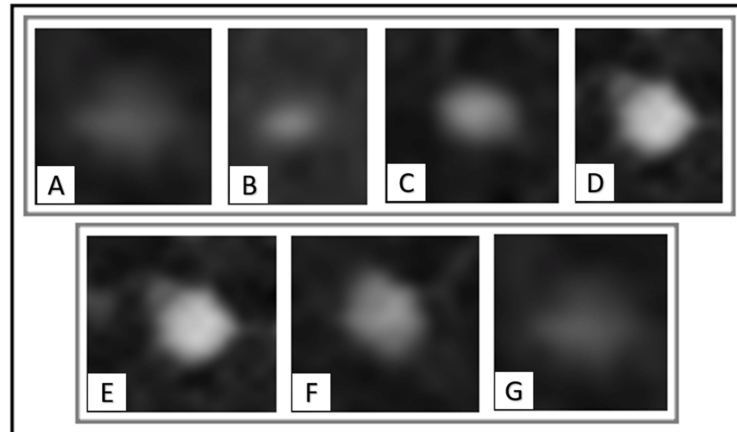


**Figure 1.** Examples of lung nodule contrast categorization ((A): very low contrast; (B): low contrast; (C): moderate contrast; (D): high contrast) and density categorization ((E): solid; (F): part-solid; (G): pure ground glass) at CT.

### 2.5. Standard of Reference

The reference standard was established in a two-step approach. First, chest CT served as a reference standard compared with PET/MR to determine the number of missed pulmonary nodules and/or false findings on MRI. Each lung nodule found on the initial chest CT dataset but not detected on  $^{18}\text{F}$ FDG-PET/MRI has been rated as a missed nodule (see Figure 2). Contrarily, each lung nodule found on  $^{18}\text{F}$ FDG-PET/MRI but not definable in chest CT was categorized as a “false-finding” (see Figure 3). The missed lung nodules in PET/MRI were categorized as benign, follow-up needed or malignant, based on CT findings. In a second step, all lesions initially categorized as follow-up needed or malignant were rated again in the follow-up examination. Follow-up imaging includes either chest CT ( $n = 27$ ), MRI ( $n = 93$ ) or both ( $n = 32$ ). The average follow-up interval for chest CT was 6.4 months (range: 2.8 to 27.5 months) and 15.5 month (range: 10 to 29 months) for a whole-body MRI.

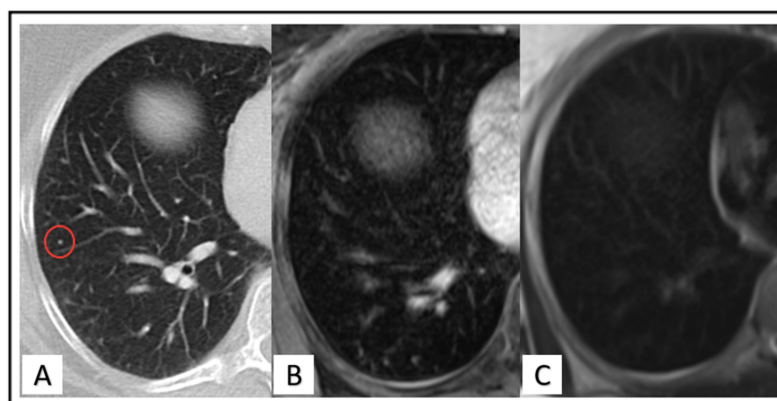


**Figure 2.** Images of a 46-year-old woman. Four-millimeter lung nodule located in right lower quadrant (red circle) identified on the CT image (A) but not recognizable in VIBE (B) nor HASTE (C) sequence.

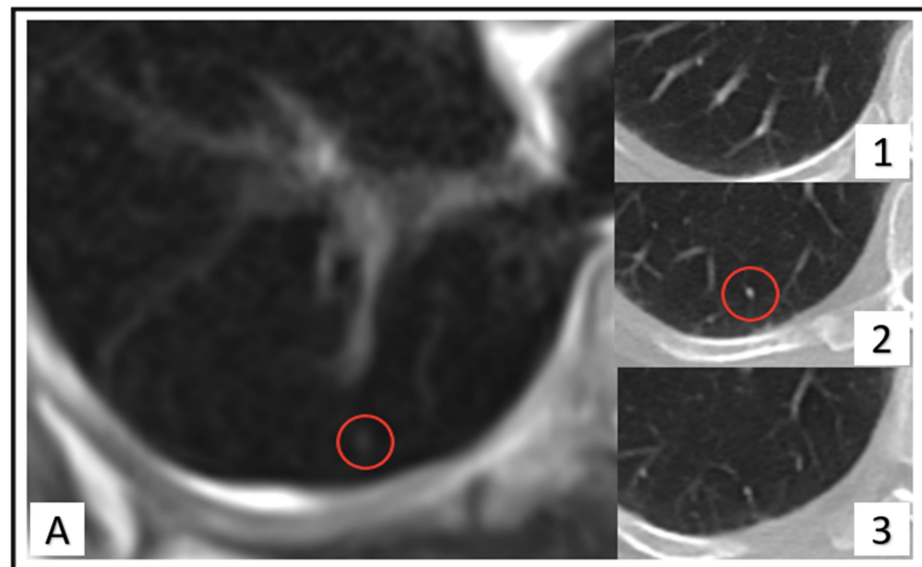


**Figure 3.** Images of a 62-year-old woman. Three-millimeter lung nodule located in right lower quadrant (red circle) identified at HASTE sequence (A) that turned out as vessel in CT (1–3), continuous structure) due to slice-thickness artifact, evaluated as false-finding.

New lung nodules at follow-up were not included in the evaluation. Missed lung nodules in MRI, that were rated as benign in initial CT or that need no further follow-up after first follow-up examination were rated as “non-relevant missing”. All missed lung nodules that were rated as malignant in initial CT or that needed further evaluation after first follow-up examination were rated as “relevant missing”. Due to clinical and ethical standards as well as the small size and localization of the evaluated lung nodules, a histological confirmation was not possible.

### 2.6. Statistical Analysis

SPSS Statistics 26 (IBM Inc., Armonk, NY, USA) was used for statistical analysis. Both patient-based and lesion-based data analysis was performed patient-based, and data are presented as mean  $\pm$  SD. Confidence intervals were calculated at 95%. Using the McNemar test, performance deviation between MRI VIBE and MRI HASTE in lung nodule delineation was analyzed.

## 3. Results

### 3.1. Patient Based Analysis

In initial CT, lung nodules were present in 84/152 (55%) of the women. Out of these 84 patients, 46 (55%) were missed in MRI VIBE, 67 (80%) in MRI HASTE, and 46 (54%) taking MRI VIBE and MRI HASTE into account. While no signs of malignancy were seen in corresponding CT in the majority of the women with missed lung nodules in MRI VIBE (70/84; 83%), a total of 14/84 (17%) of the missed women required further follow-up evaluation based on the CT information. Corresponding results were 25/84 (30%) for MRI HASTE and 14/84 (17%) for MRI HASTE and VIBE (see Table 1A). In women missed by MRI VIBE or MRI VIBE and HASTE, follow-up examinations did not reveal suspicious pulmonary nodules, while one woman missed by MRI HASTE (1%) showed a growing lung metastasis in the follow-up examination (see Table 1B). In total, 3/84 (4%) women of our cohort showed pulmonary metastases. Additionally, one woman in MRI VIBE, two women in MRI HASTE and three women in MRI VIBE and HASTE showed “false positive” findings, meaning there was a suspicious lung finding without any correlation in the CT.

**Table 1.** Patient-based analysis. (A) Classification of women with missed lung nodules at MRI VIBE, MRI HASTE and MRI VIBE and HASTE based on initial CT. (B) Classification of women with missed lung nodules at MRI VIBE, MRI HASTE and MRI VIBE and HASTE based on initial CT that needed further follow-up imaging.

(A)	Correspond to Initial CT			
	Missed Women with Lung Nodules Total	Benign Ratings	Follow-Up Needed	Sign of Malignancy
VIBE	46/84	32/84 (38%)	14/84 (17%)	0/84
HASTE	67/84	42/84 (50%)	25/84 (30%)	0/84
VIBE and HASTE	45/84	31/84 (37%)	14/84 (17%)	0/84
(B)	Correspond to Follow-Up (MRI/CT)			
	Follow-Up Needed Women Total	Benign Ratings	Further Follow-Up Needed	Sign of Malignancy
VIBE	14/84	14/84 (17%)	0/84	0/84
HASTE	25/84	24/84 (29%)	0/84	1/84 (1%)
VIBE and HASTE	14/84	14/84 (17%)	0/84	0/84

Thus, on a patients-based analysis no relevant missing occurred based on MRI VIBE or MRI VIBE and HASTE information whereas one (1/84; 1%) relevant missing occurred based on MRI HASTE information.

### 3.2. Lesion Based Analysis

A total of 163 lung nodules were present in the initial CT examinations of all women. A total of 96/163 (59%) of lung nodules were not detected in the MRI VIBE datasets and 138/163 (85%) in the MRI HASTE datasets (see Table 2A). Thus, MRI VIBE outperforms MRI HASTE in the detectability of lung nodules ( $p < 0.01$ ).

**Table 2.** Lesion-based analysis. (A) Classification of lung nodules at MRI VIBE or MRI based on initial CT. (B) Classification of lung nodules at MRI VIBE or MRI HASTE based on initial CT that needed further follow-up imaging.

(A)	Correspond to Initial CT			
	Missed Nodules Total	Benign Ratings	Follow-Up Needed	Sign of Malignancy
VIBE	96/163	59/96 (62%)	36/96 (38%)	1/96 (1%)
HASTE	138/163	74/138 (54%)	62/138 (45%)	2/138 (2%)
(B)	Correspond to Follow-Up (MRI/CT)			
	Follow-Up Needed Nodules	Benign Ratings	Further Follow-Up Needed	Sign of Malignancy
VIBE	36/96	92/96 (96%)	0	4/96 (4%)
HASTE	62/138	130/138 (94%)	0	8/138 (6%)

Out of the 96 missed lung nodules in MRI VIBE, 36 (38%) needed further follow-up evaluation, and 1 (1%) was rated as metastasis based on corresponding CT information. Follow-up examination revealed malignancy for an additional four (4%) lung nodules initially missed in MRI VIBE. In MRI HASTE a total of 62 of the 138 (45%) missed lung nodules needed further follow-up evaluation and 2 (2%) were rated as metastases based on corresponding CT information. Follow-up examination revealed malignancy for an additional eight lung nodules (6%) (see Table 2B).

Thus, on a lesion-based analysis a total, of 4/96 (4%) relevant missing lung nodules were seen in MRI VIBE and at 8/138 (6%) in MRI HASTE.

The average size of missed lung nodules was  $3.2 \text{ mm} \pm 1.2 \text{ mm}$  (range of 1–8 mm; 95% CI: 3.4–3.9 mm) at MRI VIBE and  $3.6 \text{ mm} \pm 1.4 \text{ mm}$  (range of 1–9 mm; 95% CI: 3.0–3.5 mm) at MRI HASTE (see Figure 4). Predominant location of missed lung nodules at MRI VIBE and MRI HASTE was in left lower quadrant (MRI VIBE: 30/48, 63%; MRI HASTE: 43/48, 90%) and close to the hilum (MRI VIBE: 21/21, 100%; MRI HASTE: 20/21, 95%). Lung nodules with very low contrast in CT were not detectable at MRI VIBE and MRI HASTE. Especially ground glass density was unfavorable for MRI detection rate in both sequences (MRI VIBE: 13/20, 65%; MRI HASTE: 18/20, 90%). Round shaped (MRI VIBE: 52/96, 54%; MRI HASTE: 70/138, 51%) and solid density (MRI VIBE: 54/96, 56%; MRI HASTE: 80/138, 58%) was the main characterization of missed lung nodules (see Table 3).

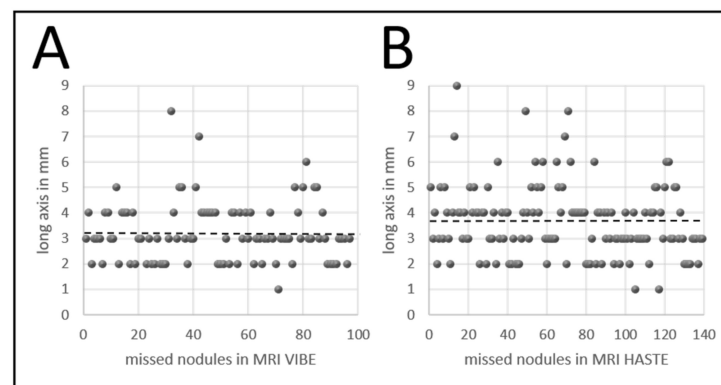


**Figure 4.** Sizes of missed lung nodules at (A) MRI VIBE ( $n = 96$ ) and (B) MRI HASTE ( $n = 138$ ) measured on initial CT. Average size (broken line) of nodules was 3.2 mm (range 1–8 mm) in MRI VIBE and 3.6 mm (range 1–9 mm) in MRI HASTE.

**Table 3.** Localization and characteristics of missed lung nodules at MRI VIBE and MRI HASTE sequence corresponding to CT.

	CT Total	VIBE	HASTE
<b>Localization (Quadrant):</b>			
1- right upper	40	23 (58%)	34 (85%)
2- left upper	23	13 (57%)	17 (74%)
3- right lower	52	30 (58%)	44 (85%)
4- left lower	48	30 (63%)	43 (90%)
<b>Localization (lung tissue):</b>			
1- pleural	53	20 (38%)	39 (74%)
2- subpleural	55	33 (60%)	47 (85%)
3- central	34	22 (65%)	32 (94%)
4- hilum	21	21 (100%)	20 (95%)
<b>Contrast:</b>			
1- very low contrast	3	3 (100%)	3 (100%)
2- low contrast	27	12 (44%)	24 (89%)
3- moderate contrast	63	41 (65%)	54 (86%)
4- high contrast	70	40 (57%)	57 (81%)
<b>Density:</b>			
1- solid	96	54 (56%)	80 (83%)
2- part-solid	47	29 (62%)	40 (85%)
3- pure ground glass	20	13 (65%)	18 (90%)
<b>Shape:</b>			
1- round	80	52 (65%)	70 (88%)
2- oval	54	27 (50%)	43 (80%)
3- ellipsoidal	14	9 (64%)	14 (100%)
4- lobular	1	1 (100%)	1 (100%)
5- notched	2	1 (50%)	1 (50%)
6- irregular	12	6 (50%)	9 (75%)

### 3.3. False Findings and Image Quality

Twenty-five additional lung nodules were detected by MRI that were not definable in CT (MRI VIBE: 10/25; MRI HASTE: 14/25; MRI VIBE and HASTE: 1/25). These were characterized as “false findings” generally consistent with a partial volume effect (e.g., vessel summation) after CT correlation. None of the “false findings” turned out to be a “true-finding” in follow-up imaging. A good image quality was achieved in both initial and follow-up imaging (see Table 4).

**Table 4.** Image quality at initial imaging and follow-up (FU) imaging according to a four-point Likert scale (1—very poor image quality to 4—excellent image quality).

	Initial Imaging	FU Imaging
Chest CT	4.0 ± 0.3 (CI: 3.9–4.0)	4.0 ± 0.3 (CI: 3.9–4.0)
MRI VIBE	3.5 ± 0.7 (CI: 3.4–3.6)	3.4 ± 0.8 (CI: 3.3–3.6)
MRI HASTE	3.6 ± 0.6 (CI: 3.5–3.7)	3.4 ± 0.7 (CI: 3.3–3.6)

## 4. Discussion

The improved therapeutic options for breast carcinoma in recent years have led to a special role of primary staging compared to other oncological diseases. While in many carcinomas, the primary therapy strongly depends on the size of the primary tumor and/or locoregional lymph node metastases, in breast cancer the tumor biology is primarily decisive for the primary therapy. The involvement of locoregional lymph nodes is also initially secondary, which is reflected in the oncologically unique term “locally advanced disease”. The aim of image-based primary staging in women with newly-diagnosed breast cancer is thus to primarily exclude distant metastases. At initial diagnosis, up to 10% of women with breast cancer have distant metastases, and especially lung metastases, increases the risk of death in the first year of illness [23]. According to previous studies, 52% to 59% of breast cancer patients show lung nodules at initial staging, underlining our results [24,25]. Thus, detecting and interpreting lung nodules is a relevant part of image-based cancer staging in radiological diagnostics, and lung CT continues to serve as the diagnostic of choice for the detection and classification of pulmonary nodules [15,26,27]. The increasing implementation of [<sup>18</sup>F]FDG-PET/MRI as a primary staging tool for breast cancer patients in a radiation-saving one-stop staging algorithm bears the risk of missing lung nodules, due to a lower sensitivity of the MRI component [11,28]. However, on the other hand, it is questionable if all missed lung nodules lead to a clinical impact or whether they would just lead to additional follow-up imaging to justify benignity. This study serves as one of the largest studies with a homogeneous non-primary metastatic patient collective to evaluate the clinical relevance of missed lung nodules in [<sup>18</sup>F]FDG-PET/MRI staging for women suffering from high-risk breast cancer, contrary to others that include more than one tumor entity with mostly known metastases [15,29,30].

According to the reference standard, no patient with clinically-relevant lung nodules was missed, but there was a small number of undetected clinically-relevant lung nodules in general. Missed lung nodules had a maximum average size of 4 mm and the evaluated data show that most of them are benign (i.e., post-infectious or indurative genesis) concordant to the results of the current literature [15,16]. Here, four (MRI VIBE) or eight (MRI HASTE) lesions were clinically relevant. However, due to the missed clinically-relevant, pulmonary nodules, there were no potential changes in treatment strategy as other clinically-relevant pulmonary nodules had already been diagnosed. In general, a neoadjuvant approach is used to treat women with locally advanced breast cancer, and this approach is followed until there is proof of distant metastases, meaning that since there is a small pulmonal lesion, there will be no switch to a palliative regimen. Thus, pulmonary staging in patients with newly-diagnosed breast cancer can be performed by [<sup>18</sup>F]FDG-PET/MRI. Concordant to previous studies, the detectability of lung lesions greater than 10 mm on PET/MRI was possibly reliable [15,26,31,32]. Taking this together, definite pulmonal metastases dependent on a size larger than 10 mm, as well as an eventual multi-focal appearance,

can be accurately detected at initial [ $^{18}\text{F}$ ]FDG-PET/MRI staging. Based on our data, there could be missed lung nodules in MRI up to a diameter of 8 mm. Thus, we think that for all breast cancer patients who were initially staged by PET/MRI, a low dose CT of the thorax should be performed after neoadjuvant system therapy has been performed. On the other hand, there is no need to perform a CT in addition to [ $^{18}\text{F}$ ]FDG-PET/MRI at initial staging, as this study shows that no lung nodules with direct clinical impact on therapy planning are missed.

Our results confirm the findings of previous studies that MRI VIBE outperforms MRI HASTE for the detection of lung nodules in breast cancer. Smaller lung nodules, especially, were not detected, caused by the higher slice thickness of MRI HASTE [12,29]. Our results support the recommendation of a T1-weighted gradient echo or pulse sequences (i.e., VIBE) for MR-based lung nodule screening with a missing rate of 59% at MRI VIBE and 85% at MRI HASTE [15,33–35]. Using newer sequences such as STAR VIBE may reduce the current missing rates [12]. Nonetheless, a relevant portion of lung nodules was missed, especially in the left lower quadrant (MRI VIBE: 63%; MRI HASTE: 90%) and nearly all close to the hilum (MRI VIBE: 100%; MRI HASTE: 95%). Additionally, lung nodules that revealed a very low contrast, as well as a pure ground glass opacity at CT, had an unsurprisingly lower detection rate. Some reasons for that are a low tissue density in the lungs, as well as rapid signal loss at the transition from lung to soft tissue, and artifacts caused by cardiac and respiratory motion, as well as small lung nodule size [12,35]. Concordant to the study of Biondetti et al. (2021), most missed lung nodules had a part-solid to solid density; furthermore, they are predominantly round shaped. Nevertheless, the MRI detectability rate decreases with lower nodule density at CT, as our data show.

Finally using [ $^{18}\text{F}$ ]FDG-PET/MRI one-stop whole-body staging algorithm, MRI VIBE sequence represents an essential sequence in lung nodule detection that should be viewed carefully; but, its lower sensitivity in detecting centrally located lung lesions should be kept in mind.

This study has some limitations. First, CT follow-up was not available for all women. However, under the assumption that lung nodules larger than 10 mm can be detected by MRI more accurately, a relevant growth should be demarcated by MRI [15,26,31,32]. A second limitation is the considerable variability in follow-up intervals. However, an optimal follow-up interval for patients generally suffering from cancer depends on the aggressiveness and doubling time of the underlying tumor histology, and therefore may vary from 6 weeks to 6 months [29,36–38]. To counteract this, the planning of follow-up examinations in this study was based on the Fleischner guidelines.

## 5. Conclusions

All women with newly-diagnosed breast cancer and clinically-relevant lung nodules showed positive detection on [ $^{18}\text{F}$ ]FDG-PET/MRI initial staging. However, due to the lower sensitivity in detecting lung nodules, a small proportion of clinically-relevant lung nodules are missed. Thus, supplemental low-dose CT of the thorax, after neoadjuvant systemic therapy has been administered, should be considered for backup.

**Author Contributions:** Conceptualization, J.K.; Data curation, K.J., N.M.B., C.J.G., J.M., F.D., C.R., A.-K.B., O.H., S.M. and H.H.Q.; Formal analysis, K.J.; Investigation, K.J. and J.K.; Methodology, J.K.; Resources, K.H., L.U. and G.A.; Supervision, K.H., L.U., G.A. and J.K.; Validation, K.J. and N.M.B.; Visualization, K.J.; Writing—original draft, K.J.; Writing—review & editing, N.M.B., C.J.G., J.M., F.D., C.R., K.H., A.-K.B., O.H., S.M., H.H.Q., L.U., G.A. and J.K. All authors have read and agreed to the published version of the manuscript.

**Funding:** The study is funded by Deutsche Forschungsgemeinschaft (DFG), the German Research Foundation (BU3075/2-1). The funding foundation was not involved in trial design, patient recruitment, data collection, analysis, interpretation or presentation, writing or editing of the reports, or the decision to submit for publication. The corresponding author had full access to all data in the study and had all responsibility for the decision to submit for publication.

**Institutional Review Board Statement:** All procedures performed were in accordance with the ethical standards of the institutional research committee of the University Duisburg-Essen (study number 17-7396-BO) and Düsseldorf (study number 6040 R) and with the principles of the 1964 Declaration of Helsinki and its later amendments. Informed consent was obtained from all individual participants included in the study.

**Informed Consent Statement:** Informed consent was obtained from all subjects involved in the study.

**Data Availability Statement:** The datasets used and/or analyzed during the current study are available from the corresponding author on reasonable request.

**Acknowledgments:** This publication contains parts of the MD thesis of Charlotte Geuting and is therefore in partial fulfillment of the requirements for an MD thesis at the Medical Faculty of the Heinrich-Heine University, Düsseldorf.

**Conflicts of Interest:** Christoph Rischpler reports a research grant from Pfizer; a consultancy for Adacap and Pfizer; and speaker honoraria from Adacap, Alnylam, BTG, GE Healthcare, Pfizer, and Siemens Healthineers outside of the submitted work. No other potential conflicts of interests relevant to this article exist. The funders had no role in the design of the study; in the collection, analyses, or interpretation of data; in the writing of the manuscript, or in the decision to publish the results.

## References

1. Bray, F.; Ferlay, J.; Soerjomataram, I.; Siegel, R.L.; Torre, L.A.; Jemal, A. Global cancer statistics 2018: GLOBOCAN estimates of incidence and mortality worldwide for 36 cancers in 185 countries. *CA Cancer J. Clin.* **2018**, *68*, 394–424. [CrossRef] [PubMed]
2. Early Breast Cancer Trialists' Collaborative Group. Trastuzumab for early-stage, HER2-positive breast cancer: A meta-analysis of 13,864 women in seven randomised trials. *Lancet Oncol.* **2021**, *22*, 1139–1150. [CrossRef]
3. Gallagher, C.M.; More, K.; Masaquel, A.; Kamath, T.; Guérin, A.; Ionescu-Iltu, R.; Nitulescu, R.; Gauthier-Loiselle, M.; Sicignano, N.; Butts, E.; et al. Survival in patients with non-metastatic breast cancer treated with adjuvant trastuzumab in clinical practice. *Springerplus* **2016**, *5*, 395. [CrossRef]
4. Leitlinienprogramm Onkologie (Deutsche Krebsgesellschaft DK, AWMF). S3-Leitlinie Früherkennung, Diagnose, Therapie und Nachsorge des Mammakarzinoms. Version 4.4. 2021. Available online: [https://www.leitlinienprogramm-onkologie.de/fileadmin/user\\_upload/Downloads/Leitlinien/Mammakarzinom\\_4\\_0/Version\\_4.4/LL\\_Mammakarzinom\\_Kurzversion\\_4.3.pdf](https://www.leitlinienprogramm-onkologie.de/fileadmin/user_upload/Downloads/Leitlinien/Mammakarzinom_4_0/Version_4.4/LL_Mammakarzinom_Kurzversion_4.3.pdf) (accessed on 7 June 2022).
5. Groheux, D.; Hindie, E. Breast cancer: Initial workup and staging with FDG PET/CT. *Clin. Transl. Imaging* **2021**, *9*, 221–231. [CrossRef] [PubMed]
6. Ulaner, G.A.; Castillo, R.; Goldman, D.A.; Wills, J.; Riedl, C.; Pinker-Domenig, K.; Jochelson, M.S.; Gönen, M. <sup>18</sup>F-FDG-PET/CT for systemic staging of newly diagnosed triple-negative breast cancer. *Eur. J. Nucl. Med. Mol. Imaging* **2016**, *43*, 1937–1944. [CrossRef]
7. Ulaner, G.A.; Castillo, R.; Wills, J.; Gönen, M.; Goldman, D.A. <sup>18</sup>F-FDG-PET/CT for systemic staging of patients with newly diagnosed ER-positive and HER2-positive breast cancer. *Eur. J. Nucl. Med. Mol. Imaging* **2017**, *44*, 1420–1427. [CrossRef]
8. Bruckmann, N.M.; Kirchner, J.; Morawitz, J.; Umutlu, L.; Herrmann, K.; Bittner, A.-K.; Hoffmann, O.; Mohrmann, S.; Ingenwerth, M.; Schaarschmidt, B.M.; et al. Prospective comparison of CT and <sup>18</sup>F-FDG PET/MRI in N and M staging of primary breast cancer patients: Initial results. *PLoS ONE* **2021**, *16*, e0260804. [CrossRef]
9. Bruckmann, N.M.; Kirchner, J.; Umutlu, L.; Fendler, W.P.; Seifert, R.; Herrmann, K.; Bittner, A.-K.; Hoffmann, O.; Mohrmann, S.; Antke, C.; et al. Prospective comparison of the diagnostic accuracy of <sup>18</sup>F-FDG PET/MRI, MRI, CT, and bone scintigraphy for the detection of bone metastases in the initial staging of primary breast cancer patients. *Eur. Radiol.* **2021**, *31*, 8714–8724. [CrossRef]
10. Sawicki, L.M.; Grueneisen, J.; Schaarschmidt, B.M.; Buchbender, C.; Nagarajah, J.; Umutlu, L.; Antoch, G.; Kinner, S. Evaluation of <sup>18</sup>F-FDG PET/MRI, <sup>18</sup>F-FDG PET/CT, MRI, and CT in whole-body staging of recurrent breast cancer. *Eur. J. Radiol.* **2016**, *85*, 459–465. [CrossRef]
11. Melsaether, A.N.; Raad, R.A.; Pujara, A.C.; Ponzio, F.D.; Pysarenko, K.M.; Jhaveri, K.; Babb, J.S.; Sigmund, E.E.; Kim, S.G.; Moy, L.A. Comparison of Whole-Body (18)F FDG PET/MR Imaging and Whole-Body (18)F FDG PET/CT in Terms of Lesion Detection and Radiation Dose in Patients with Breast Cancer. *Radiology* **2016**, *281*, 193–202. [CrossRef]
12. Bruckmann, N.M.; Kirchner, J.; Morawitz, J.; Umutlu, L.; Fendler, W.P.; Herrmann, K.; Bittner, A.-K.; Hoffmann, O.; Fehm, T.; Lindemann, M.E.; et al. Free-breathing 3D Stack of Stars GRE (StarVIBE) sequence for detecting pulmonary nodules in <sup>18</sup>F-FDG PET/MRI. *EJNMMI Phys.* **2022**, *9*, 11. [CrossRef] [PubMed]
13. Wielpütz, M.O. MRI of Pulmonary Nodules: Closing the Gap on CT. *Radiology* **2022**, *302*, 707–708. [CrossRef] [PubMed]
14. Rauscher, I.; Eiber, M.; Fürst, S.; Souvatzoglou, M.; Nekolla, S.G.; Ziegler, S.I.; Rummeny, E.J.; Schwaiger, M.; Beer, A.J. PET/MR Imaging in the Detection and Characterization of Pulmonary Lesions: Technical and Diagnostic Evaluation in Comparison to PET/CT. *J. Nucl. Med.* **2014**, *55*, 724–729. [CrossRef]

15. Sawicki, L.M.; Grueneisen, J.; Buchbender, C.; Schaarschmidt, B.M.; Gomez, B.; Ruhlmann, V.; Umutlu, L.; Antoch, G.; Heusch, P. Evaluation of the Outcome of Lung Nodules Missed on  $^{18}\text{F}$ -FDG PET/MRI Compared with  $^{18}\text{F}$ -FDG PET/CT in Patients with Known Malignancies. *J. Nucl. Med.* **2016**, *57*, 15–20. [[CrossRef](#)] [[PubMed](#)]
16. Benjamin, M.S.; Drucker, E.A.; McLoud, T.C.; Shepard, J.-A.O. Small Pulmonary Nodules: Detection at Chest CT and Outcome. *Radiology* **2003**, *226*, 489–493. [[CrossRef](#)] [[PubMed](#)]
17. Bueno, J.; Landeras, L.; Chung, J.H. Updated Fleischner Society Guidelines for Managing Incidental Pulmonary Nodules: Common Questions and Challenging Scenarios. *RadioGraphics* **2018**, *38*, 1337–1350. [[CrossRef](#)]
18. Association, W.M. World Medical Association Declaration of Helsinki: Ethical Principles for Medical Research Involving Human Subjects. *JAMA* **2013**, *310*, 2191–2194. [[CrossRef](#)]
19. Cardoso, F.; Paluch-Shimon, S.; Senkus, E.; Curigliano, G.; Aapro, M.S.; André, F.; Barrios, C.H.; Bergh, J.; Bhattacharyya, G.S.; Biganzoli, L.; et al. 5th ESO-ESMO international consensus guidelines for advanced breast cancer (ABC 5). *Ann. Oncol.* **2020**, *31*, 1623–1649. [[CrossRef](#)]
20. Cardoso, F.; Senkus, E.; Costa, A.; Papadopoulos, E.; Aapro, M.; André, F.; Harbeck, N.; Aguilar Lopez, B.; Barrios, C.H.; Bergh, J.; et al. 4th ESO-ESMO International Consensus Guidelines for Advanced Breast Cancer (ABC 4). *Ann. Oncol.* **2018**, *29*, 1634–1657. [[CrossRef](#)]
21. Kirchner, J.; Grueneisen, J.; Martin, O.; Oehmigen, M.; Quick, H.H.; Bittner, A.-K.; Hoffmann, O.; Ingenwerth, M.; Catalano, O.A.; Heusch, P.; et al. Local and whole-body staging in patients with primary breast cancer: A comparison of one-step to two-step staging utilizing  $^{18}\text{F}$ -FDG-PET/MRI. *Eur. J. Nucl. Med. Mol. Imaging* **2018**, *45*, 2328–2337. [[CrossRef](#)]
22. Rausch, I.; Quick, H.H.; Cal-Gonzalez, J.; Sattler, B.; Boellaard, R.; Beyer, T. Technical and instrumentational foundations of PET/MRI. *Eur. J. Radiol.* **2017**, *94*, A3–A13. [[CrossRef](#)] [[PubMed](#)]
23. Ording, A.G.; Heide-Jørgensen, U.; Christiansen, C.F.; Nørgaard, M.; Acquavella, J.; Sørensen, H.T. Site of metastasis and breast cancer mortality: A Danish nationwide registry-based cohort study. *Clin. Exp. Metastasis* **2017**, *34*, 93–101. [[CrossRef](#)] [[PubMed](#)]
24. Daglar, G.; Yuksek, Y.N.; Gozalan, U.; Tutuncu, T.; Kama, N.A. The significance of pulmonary nodule in breast cancer patients. *Bratisl. Lek. Listy* **2010**, *111*, 280–283. [[PubMed](#)]
25. Li, F.; Armato, S.G.; Giger, M.L.; MacMahon, H. Clinical significance of noncalcified lung nodules in patients with breast cancer. *Breast Cancer Res. Treat.* **2016**, *159*, 265–271. [[CrossRef](#)]
26. Sommer, G.; Tremper, J.; Koenigkam-Santos, M.; Delorme, S.; Becker, N.; Biederer, J.; Kauczor, H.-U.; Heussel, C.P.; Schlemmer, H.-P.; Puderbach, M. Lung nodule detection in a high-risk population: Comparison of magnetic resonance imaging and low-dose computed tomography. *Eur. J. Radiol.* **2014**, *83*, 600–605. [[CrossRef](#)]
27. Biederer, J.; Hintze, C.; Fabel, M. MRI of pulmonary nodules: Technique and diagnostic value. *Cancer Imaging* **2008**, *8*, 125–130. [[CrossRef](#)]
28. Evangelista, L.; Cuppari, L.; Burei, M.; Zorz, A.; Caumo, F. Head-to-head comparison between  $^{18}\text{F}$ -FDG PET/CT and PET/MRI in breast cancer. *Clin. Transl. Imaging* **2019**, *7*, 99–104. [[CrossRef](#)]
29. Biondetti, P.; Vangel, M.G.; Lahoud, R.M.; Furtado, F.S.; Rosen, B.R.; Groshar, D.; Canamaque, L.G.; Umutlu, L.; Zhang, E.W.; Mahmood, U.; et al. PET/MRI assessment of lung nodules in primary abdominal malignancies: Sensitivity and outcome analysis. *Eur. J. Nucl. Med. Mol. Imaging* **2021**, *48*, 1976–1986. [[CrossRef](#)]
30. Raad, R.A.; Friedman, K.P.; Heacock, L.; Ponzio, F.; Melsaether, A.; Chandarana, H. Outcome of small lung nodules missed on hybrid PET/MRI in patients with primary malignancy. *J. Magn. Reson. Imaging* **2016**, *43*, 504–511. [[CrossRef](#)]
31. Chandarana, H.; Heacock, L.; Rakheja, R.; DeMello, L.R.; Bonavita, J.; Block, T.K.; Geppert, C.; Babb, J.S.; Friedman, K.P. Pulmonary Nodules in Patients with Primary Malignancy: Comparison of Hybrid PET/MR and PET/CT Imaging. *Radiology* **2013**, *268*, 874–881. [[CrossRef](#)]
32. Müller, N.L.; Gamsu, G.; Webb, W.R. Pulmonary nodules: Detection using magnetic resonance and computed tomography. *Radiology* **1985**, *155*, 687–690. [[CrossRef](#)] [[PubMed](#)]
33. Regier, M.; Kandel, S.; Kaul, M.G.; Hoffmann, B.; Ittrich, H.; Bansmann, P.M.; Kemper, J.; Nolte-Ernsting, C.; Heller, M.; Adam, G.; et al. Detection of small pulmonary nodules in high-field MR at 3 T: Evaluation of different pulse sequences using porcine lung explants. *Eur. Radiol.* **2007**, *17*, 1341–1351. [[CrossRef](#)] [[PubMed](#)]
34. Schäfer, J.; Vollmar, J.; Schick, F.; Seemann, M.; Kamm, P.; Erdtmann, B.; Claussen, C. Detection of pulmonary nodules with breath-hold magnetic resonance imaging in comparison with computed tomography. *Rofo* **2005**, *177*, 41–49. [[CrossRef](#)] [[PubMed](#)]
35. Kumar, S.; Rai, R.; Stemmer, A.; Josan, S.; Holloway, L.; Vinod, S.; Moses, D.; Liney, G. Feasibility of free breathing Lung MRI for Radiotherapy using non-Cartesian k-space acquisition schemes. *Br. J. Radiol.* **2017**, *90*, 20170037. [[CrossRef](#)] [[PubMed](#)]
36. National Collaborating Centre for Cancer. *National Institute for Health and Clinical Excellence: Guidance; The Diagnosis and Treatment of Lung Cancer (Update)*; National Collaborating Centre for Cancer (UK): Cardiff, UK, 2011.
37. Colt, H.G.; Murgu, S.D.; Korst, R.J.; Slatore, C.G.; Unger, M.; Quadrelli, S. Follow-up and surveillance of the patient with lung cancer after curative-intent therapy: Diagnosis and management of lung cancer, 3rd ed: American College of Chest Physicians evidence-based clinical practice guidelines. *Chest* **2013**, *143*, e437S–e454S. [[CrossRef](#)]
38. Koh, W.-J.; Greer, B.E.; Abu-Rustum, N.R.; Campos, S.M.; Cho, K.; Chon, H.S.; Chu, C.; Cohn, D.; Crispens, M.A.; Dizon, D.S.; et al. Vulvar Cancer, Version 1.2017, NCCN Clinical Practice Guidelines in Oncology. *J. Natl. Compr. Cancer Netw.* **2017**, *15*, 92–120. [[CrossRef](#)]